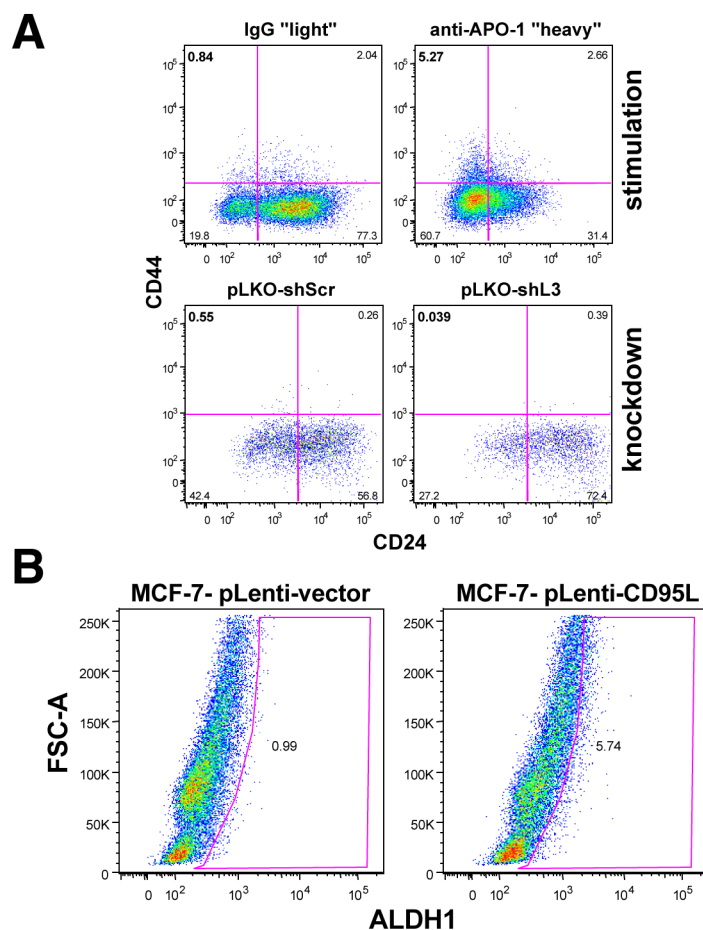


**Supplementary Information****CD95/Fas Increases Stemness in Cancer Cells by Inducing a  
STAT1 Dependent Type I Interferon Response**

Abdul S. Qadir, Paolo Ceppi, Sonia Brockway, Calvin Law, Liang Mu, Nikolai N. Khodarev, Jung Kim, Jonathan C. Zhao, William Putzbach, Andrea E. Murmann, Zhuo Chen, Wenjing Chen, Xia Liu, Arthur R. Salomon, Huiping Liu, Ralph R. Weichselbaum, Jindan Yu, and Marcus E. Peter

## Supplemental Figures and Legends



**Figure S1, related to Figure 1. Stimulation of MCF-7 cells through CD95 increases stemness markers and induces phosphorylation of STAT1.**

(A) CD44/CD24 surface staining of MCF-7 cells labeled with either light or heavy amino acids for SILAC. Cells were either treated with IgG3/anti-APO-1 for 14 days or stained 12 days after infecting cells with pLKO-shCD95L or control pLKO-shScr vector.

(B) ALDH1 activity in MCF-7 cells infected with either pLenti control or pLenti-CD95L.

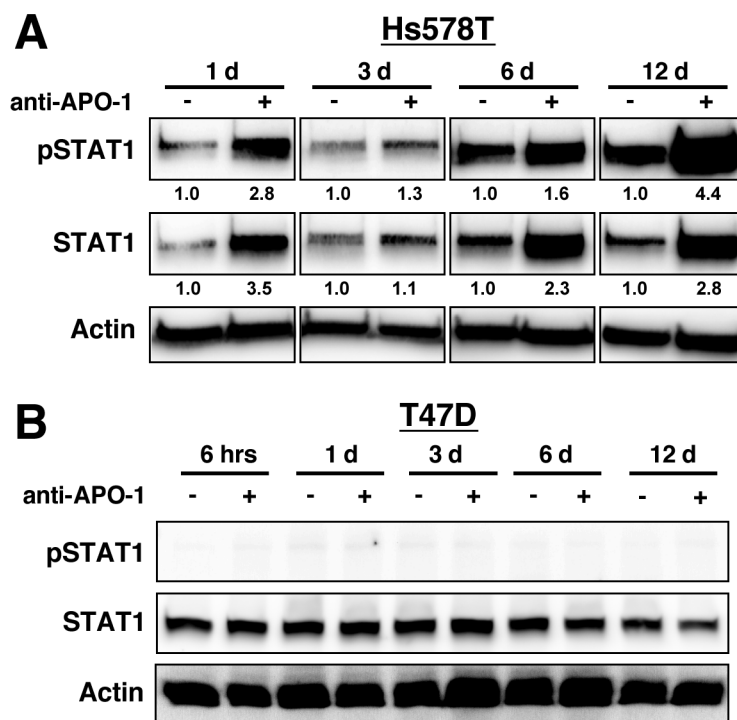


**Figure S2, related to Figure 2. Activation of STAT1 in breast cancer cell lines.**

(A) Western blot analysis of Hs578T cells treated with either IgG3 (-) or anti-APO-1 (+). Quantification of bands normalized to actin is given.

(B) Western blot analysis of T47D cells treated with either IgG3 (-) or anti-APO-1 (+).

A

up (>1.0 log2) (117)					down (>-1.0 log2) (33)
ADORA1	HERC5	LARGE	RNASEH2A	ABCC3	
ANKRD18A	<b>HERC6</b>	LGALS3BP	RPLP1	ACTA2	
ANXA2P1	HIST2H2AA3	LOC728026	SAMD9	ALDH1A3	
ATF3	H1A-A	LTB	SERHL	AMY1C	
B2M	H1A-B	MYF5	SLAH2	ARNT2	
BOLA2	H1A-E	NFKB1A	SOD2	BCAS1	
BRWD1	H1A-F	NLRP7	SP110	C9orf169	
BST2	H1A-G	NOP56	SPTS5B	CAMK2N1	
BTNGA3	H1A-H	NTN1	SSBP4	CEACAM6	
BZRAP1	HMG2B	NUPR1	SSTR1	EPAS1	
C11orf87	HSPA1A	OAS1	<b>STAT1</b>	FAM174B	
C17orf69	IR27	OAS2	TAP1	FCB	
C19orf66	IR35	OAS3	TFF3	GPRC5A	
CDC81	IR44	OASL	TSZH3	H19	
CCL5	IR44L	OAZ3	TXNIP	IDS	
CMAHP	IR6	PARP10	UBE2L6	KIAA1199	
CST8	IR16	PARP12	<b>USP18</b>	LIMCH1	
C15L3	IR17	PARP14	ZAN	LXN	
DDX60	IR12	PARP9		MMP2L2	
DNMT3B	IR13	PI4K2A		NAV2	
E1F2AK2	IR17M1	PKIB		NDRG1	
EXOC3L2	IR17M2	PLAG1		PAPSS2	
FAM63A	IR17M3	PLD6		PLA2G10	
FAM65B	IR17B1	<b>PLSCR1</b>		PMEPA1	
FBXO32	IL28A	PMAI1		PPH1BP2	
FL40448	IL28B	POTEE		PRR15L	
FLT1	IL29	PPP1R15A		RPS21	
GFRAL	IR61	PRICK2B5		S100P	
GREB1	IR67	PSMB9		SHP11	
GSTA2	ISG15	PTMA		SYTL2	
H1FX	ISG20	RAB24		TSC2-203	
HCG4	KIAA1324	RARRES3		TXNDC12	
HCP5	KLF4	RN75K		UQCRRP1	

B

ID	Name	Type	Cell line	Time	Dose	Connectivity score	Up score	Down score
CMAP-L158	<b>IFNA</b>	Ligation	BT20	6 h	100 ng/μL	0.7438	0.9275	-0.5601
CMAP-L163	<b>IFNG</b>	Ligation	MCF10A	6 h	1 ng/μL	0.7316	0.9028	-0.5604
ccsbbroad304_05881	BC12L2	Overexpression	MCF7	96 h	2 μL	0.7185	0.9001	-0.5369
ccsbbroad304_05152	SSBP4	Overexpression	MCF7	96 h	2 μL	0.7168	0.8049	-0.6288
CMAP-L163	<b>IFNG</b>	Ligation	MCF7	3 h	100 ng/μL	0.7127	0.7987	-0.6266
CMAP-L158	<b>IFNA</b>	Ligation	BT20	6 h	100 ng/μL	0.7096	0.9329	-0.4864
CMAP-L158	<b>IFNA</b>	Ligation	MCF10A	6 h	100 ng/μL	0.7073	0.9222	-0.4923
CMAP-L163	<b>IFNG</b>	Ligation	SKBR3	6 h	100 ng/μL	0.7024	0.8782	-0.5267
ccsbbroad304_07531	TANK	Overexpression	HA1E	96 h	1 μL	0.6992	0.8541	-0.5444
CMAP-L163	<b>IFNG</b>	Ligation	SKBR3	24 h	100 ng/μL	0.697	0.9153	-0.4787
CMAP-L163	<b>IFNG</b>	Ligation	SKBR3	6 h	100 ng/μL	0.6961	0.842	-0.5502
CMAP-HSF-ZNF213	ZNF213	Overexpression	HEK293T	48 h	-	0.6953	0.7885	-0.6021
CMAP-L163	<b>IFNG</b>	Ligation	MCF7	6 h	100 ng/μL	0.6949	0.9214	-0.4684
CMAP-L158	<b>IFNA</b>	Ligation	BT20	6 h	1 ng/μL	0.6948	0.8561	-0.5335
CMAP-L163	<b>IFNG</b>	Ligation	MCF10A	6 h	100 ng/μL	0.6919	0.8362	-0.5475
ccsbbroad304_05528	TICAM2	Overexpression	MCF7	96 h	2 μL	0.6917	0.818	-0.5653
CMAP-L163	<b>IFNG</b>	Ligation	H5578T	24 h	100 ng/μL	0.6908	0.9072	-0.4743
CMAP-L158	<b>IFNA</b>	Ligation	SKBR3	24 h	100 ng/μL	0.6889	0.9434	-0.4344
CMAP-L163	<b>IFNG</b>	Ligation	BT20	3 h	100 ng/μL	0.6886	0.8744	-0.5028
ccsbbroad304_00259	CD40	Overexpression	HT29	96 h	2 μL	0.6868	0.935	-0.4386
ccsbbroad304_05881	BC12L2	Overexpression	HCC515	96 h	4 μL	0.6858	0.8081	-0.5634
ETV6-PDG FRA	ETV6-PDG FRA	Overexpression	HEK293T	48 h	150 ng	0.6844	0.8336	-0.5353
ccsbbroad304_01688	TNFRSF1A	Overexpression	MCF7	96 h	2 μL	0.6836	0.8578	-0.5094
ccsbbroad304_00496	ELF4	Overexpression	MCF7	96 h	2 μL	0.6785	0.9007	-0.4564
CMAP-L158	<b>IFNA</b>	Ligation	MCF7	24 h	100 ng/μL	0.6783	0.8959	-0.4607

C

ID	Name	Type	Cell line	Time	Dose	Connectivity score	Up score	Down score	Cancer Type
CMAP-CYT-SRP3058	IFNG	Ligation	HA1E	4 h	10 ng/ml	0.6724	0.7962	-0.5486	HEK
ccsbbroad304_06429	IFNA10	Overexpression	PC3	48 h	2 μL	0.6724	0.9339	-0.4108	Prostate
CMAP-CYT-I4401	IFNA13	Ligation	HA1E	4 h	0.5 ng/ml	0.651	0.8498	-0.4523	HEK
CMAP-CYT-SRP3058	IFNG	Ligation	A549	4 h	10 ng/ml	0.6361	0.8219	-0.4502	Lung
ccsbbroad304_00833	IFNG	Overexpression	HEPG2	96 h	2 μL	0.6344	0.844	-0.4248	Liver
ccsbbroad304_06429	IFNA10	Overexpression	A375	72 h	2 μL	0.63	0.9197	-0.3403	Melanoma
ccsbbroad304_06429	IFNA10	Overexpression	PC3	96 h	2 μL	0.6183	0.9083	-0.3284	Prostate
CMAP-CYT-I4401	IFNA13	Ligation	PC3	2 h	0.5 ng/ml	0.6115	0.7791	-0.4438	Prostate
CMAP-CYT-I4401	IFNA13	Ligation	HEPG2	4 h	0.5 ng/ml	0.6052	0.8211	-0.3893	Liver
ccsbbroad304_06429	IFNA10	Overexpression	A375	48 h	2 μL	0.5998	0.9086	-0.2909	Melanoma
CMAP-CYT-SRP3058	IFNG	Ligation	VCAP	4 h	10 ng/ml	0.5874	0.7805	-0.3942	Prostate
ccsbbroad304_00832	IFNB1	Overexpression	HEPG2	96 h	2 μL	0.5757	0.8518	-0.2996	Liver
CMAP-CYT-SRP3058	IFNG	Ligation	HEPG2	4 h	10 ng/ml	0.5732	0.7741	-0.3723	Liver
ccsbbroad304_00833	IFNG	Overexpression	HCC515	96 h	4 μL	0.5556	0.91	-0.2011	Lung
ccsbbroad304_00833	IFNG	Overexpression	HT29	96 h	2 μL	0.5538	0.8736	-0.2341	Colon
ccsbbroad304_06429	IFNA10	Overexpression	A375	96 h	2 μL	0.5531	0.877	-0.2293	Melanoma
IFNA2	IFNA2	Ligation	A549	2 h	1 ng/ml	0.5506	0.7477	-0.3534	Lung
ccsbbroad304_00833	IFNG	Overexpression	VCAP	96 h	3 μL	0.5477	0.838	-0.2573	Prostate
IFNG	IFNG	Ligation	HCC515	2 h	10 ng/ml	0.5454	0.6811	-0.4097	Lung
IFNA13	IFNA13	Ligation	VCAP	4 h	0.5 ng/ml	0.5396	0.8112	-0.268	Prostate
IFNG	IFNG	Ligation	A549	2 h	10 ng/ml	0.5351	0.6513	-0.4189	Lung
CMAP-CYT-SRP3058	IFNG	Ligation	HCC515	4 h	10 ng/ml	0.5345	0.688	-0.3809	Lung
IFNG	IFNG	Ligation	VCAP	4 h	10 ng/ml	0.5342	0.7971	-0.2713	Prostate
CMAP-CYT-SRP3058	IFNG	Ligation	HT29	4 h	10 ng/ml	0.534	0.7146	-0.3534	Colon
CMAP-CYT-SRP4594	IFNA2	Ligation	VCAP	2 h	1 ng/ml	0.5327	0.6165	-0.4489	Prostate
IFNG	IFNG	Ligation	HT29	2 h	10 ng/ml	0.5146	0.6966	-0.3326	Colon

**Figure S3, related to Figure 3: Linccloud analysis of the genes deregulated in MCF-7 cells treated with anti-APO-1 for 14 days.**

(A) List of up and downregulated genes that were used for the analysis.

(B) List of the top 25 gene signatures that were most similar to the up- and downregulated genes in cells stimulated through CD95, ranked according to highest connectivity score. Gene signatures that were obtained after treating cells with IFNs are in red.

(C) List of top 25 gene signatures that followed the 25 signatures in B and that involved treatments with IFNs, ranked according to highest connectivity score.

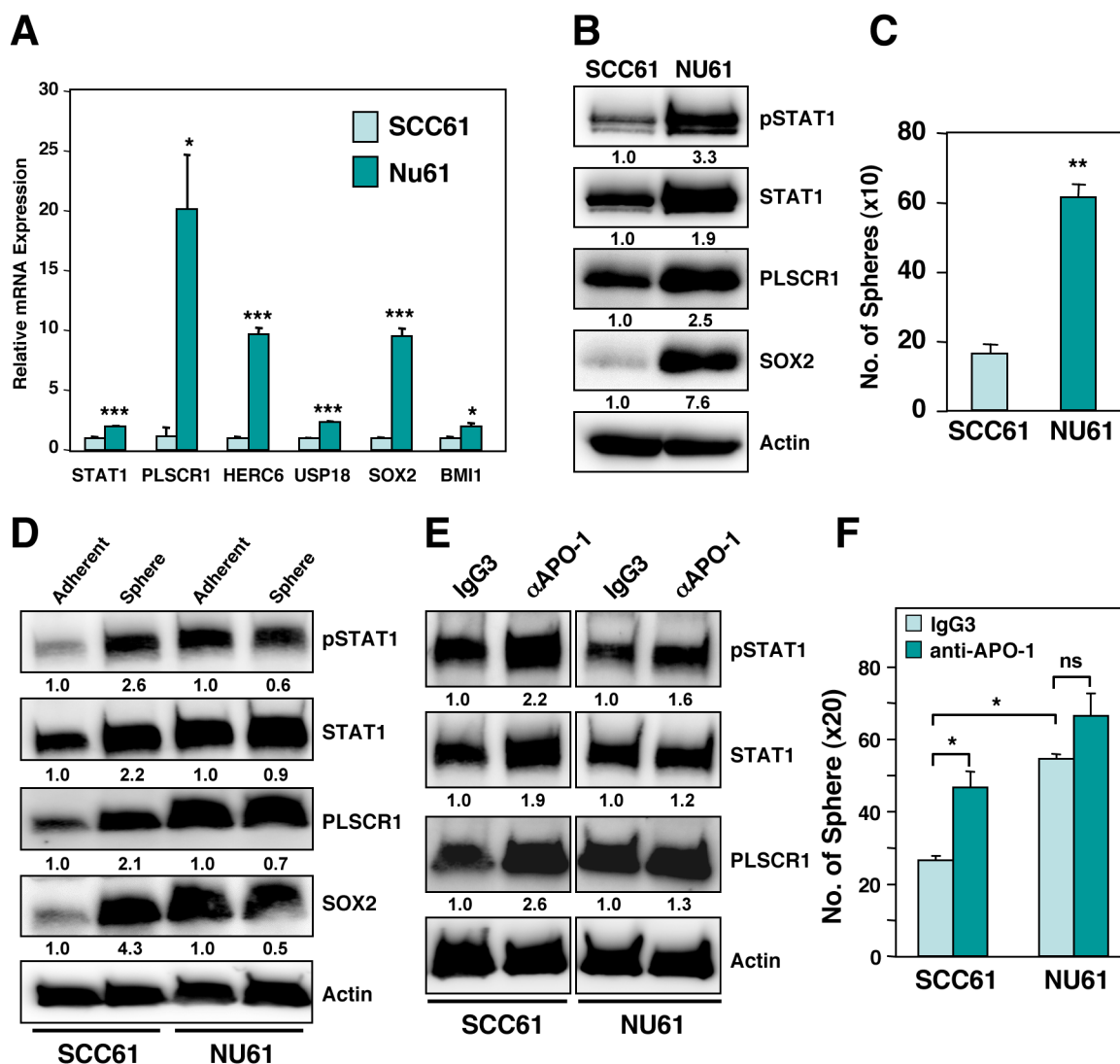


**Figure S4, related to Figure 4: STAT1 is phosphorylated and upregulated in SCC61 cancer stem cells and in the radiation resistant variant Nu61.**

(A) Real-time PCR analysis of STAT1 target genes and stem cell marker genes SOX2 and BMI1 in SCC61 and Nu61 cells.

(B) Western blot analysis of SCC61 and Nu61 cells.

(C) Sphere forming assay of SCC61 and Nu61 cells.

(D) Western blot analysis of SCC61 and Nu61 cells grown adherent or under sphere forming conditions.

(E) Western blot analysis of SCC61 and Nu61 cells treated with either IgG3 or anti-APO-1 for 4 days in the presence of zVAD.

(F) Sphere forming assay of SCC61 and Nu61 cells treated with either IgG3 or anti-APO-1 for 4 days. p-value \* $<0.05$ , \*\* $<0.001$ ; \*\*\* $<0.0001$ ; ns, not significant.

Quantification of bands normalized to actin is given.

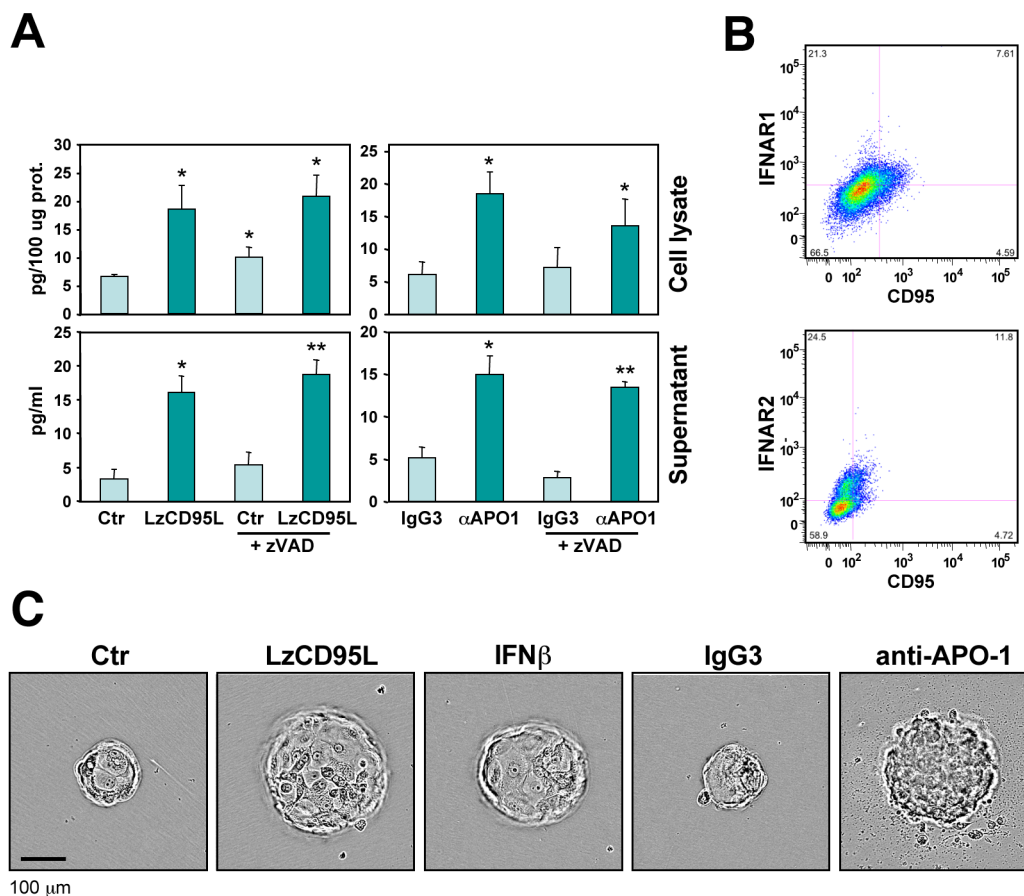


**Figure S5, related to Figure 5: CD95 mediated induction of IFN $\alpha$  is not dependent on caspase activation.**

(A) ELISA quantification of IFN $\alpha$  produced by MCF-7 cells untreated or treated with LzCD95L for two days in the absence or presence of zVAD. p-value  $* < 0.05$ ,  $** < 0.001$ ; p-values were calculated compared to no zVAD control.

(B) Surface staining of MCF-7 cells for CD95 and IFNAR1 (top) or IFNAR2 (bottom).

(C) Representative images of spheres formed after plating MCF-7 cells (untreated (Ctr) or treated with either LzCD95L, IFN $\beta$ , IgG3, or anti-APO-1 for 6 days) at one cell per well in 96-well plates.

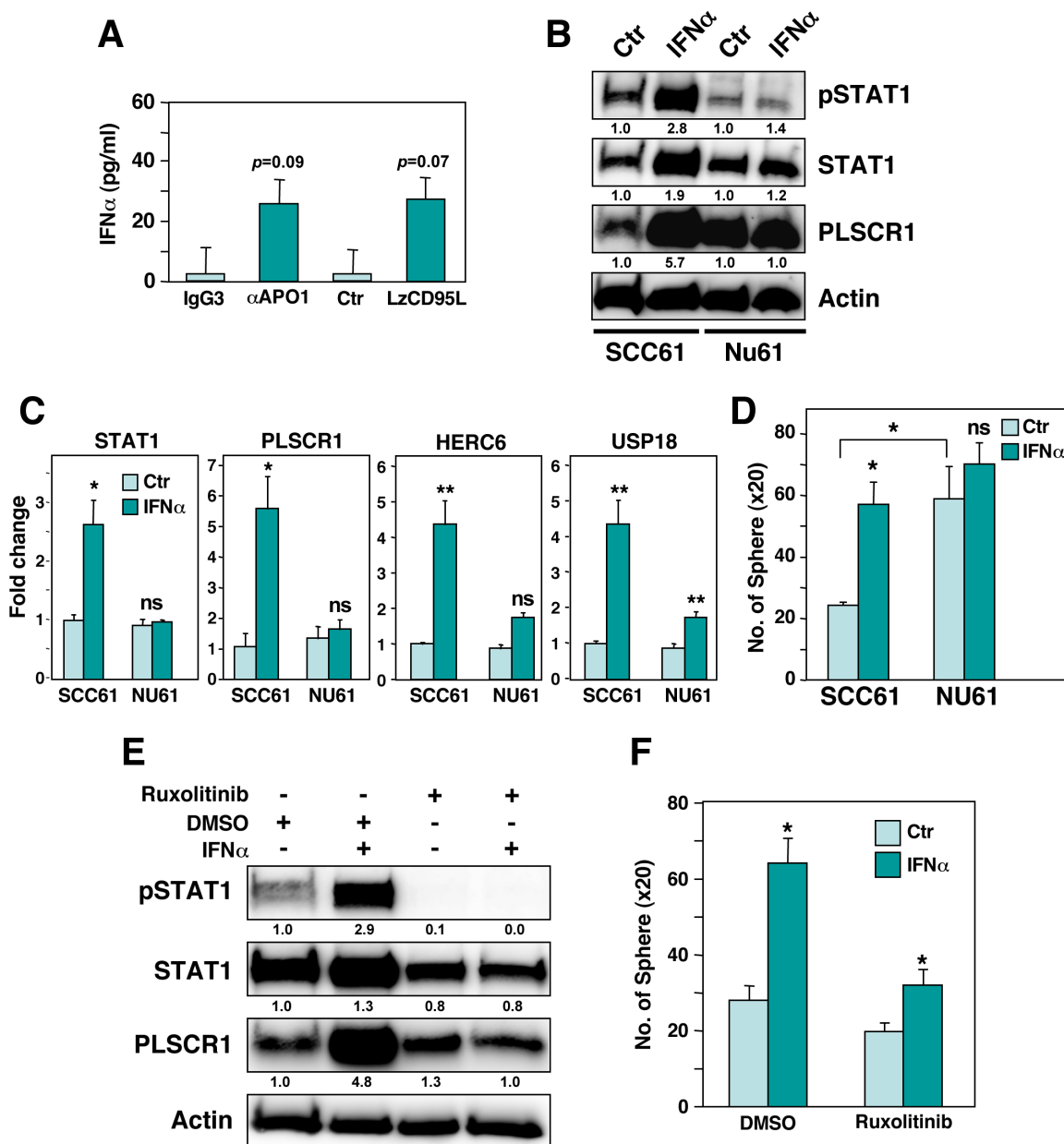


**Figure S6, related to Figure 5: CD95 stimulation induces IFN $\alpha$  in SCC61 cells and IFN $\alpha$  increases stemness in SCC61 but not in Nu61 cells.**

(A) ELISA quantification of IFN $\alpha$  produced by SCC61 cells treated with either IgG3, anti-APO-1 or LzCD95L for 2 days.

(B) Western blot analysis of SCC61 or Nu61 cells control treated or treated with IFN $\alpha$  for 4 days. Quantification of bands normalized to actin is given.

(C) Real-time PCR quantification of STAT1 mRNA and the mRNAs of the three STAT1 regulated genes.

(D) Sphere formation of SCC61 and Nu61 cells treated as in B.

(E) Western blot analysis of SCC61 cells treated with either IgG3 or anti-APO-1 for 4 days and DMSO solvent control or Ruxolitinib. Quantification of bands normalized to actin is given.

(F) Sphere formation of SCC61 cells treated as in E. p-value \* $<0.05$ , \*\* $<0.001$ ; \*\*\* $<0.0001$ ; ns, not significant. Quantification of bands normalized to actin is given.

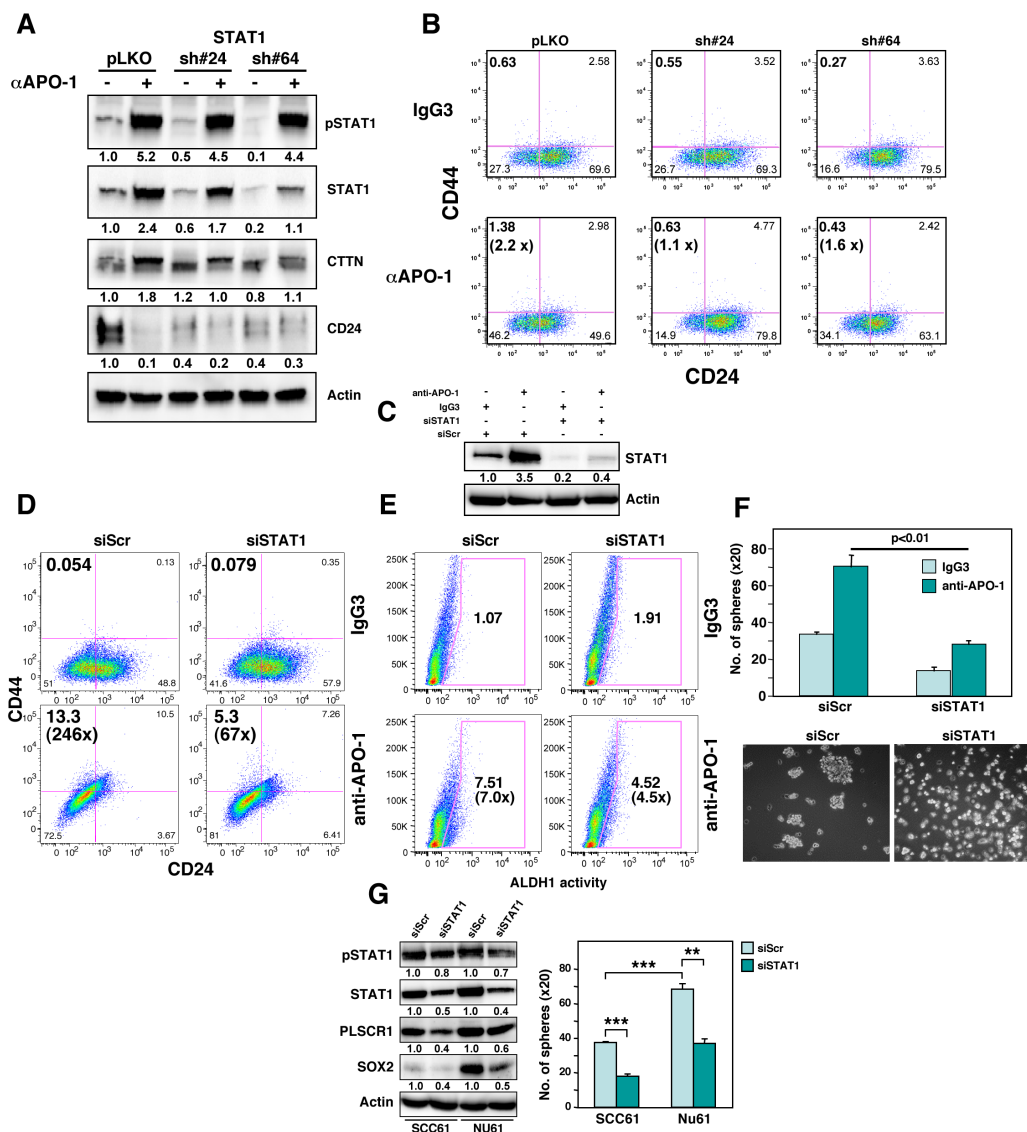


**Figure S7, related to Figure 6: Knockdown of STAT1 reduces the ability of CD95 to mediate cancer stemness.**

(A) Western blot analysis of MCF-7 cells infected with control shRNA expressing lentivirus (pLKO) or with two different shRNAs targeting STAT1 and incubated with either IgG3 (-) or anti-APO-1 (+) for 12 days. Quantification of bands normalized to actin is given.

(B) CD44/CD24 surface staining of the cells in A (treated with IgG3 or anti-APO-1 for 6 days).

(C) Western blot analysis of MCF-7 cells treated with either IgG3 or anti-APO-1 for 4 days following knockdown of STAT1 or transfection with a nontargeting siRNA (siScr). Quantification of bands normalized to actin is given.

(D) CD44/CD24 surface staining of MCF-7 cells treated with either IgG3 or anti-APO-1 for 7 days and transfection with either siScr or siSTAT1 at day 0 and at day 3.

(E, F) ALDH1 and sphere forming activity of the cells in D.

(G) Western blot analysis (left) and sphere formation assay (right) of SCC61 and Nu61 cells after transfection with either siSTAT1 or a siScr. Quantification of bands normalized to actin is given. p-value \*\*<0.001; \*\*\*<0.0001.



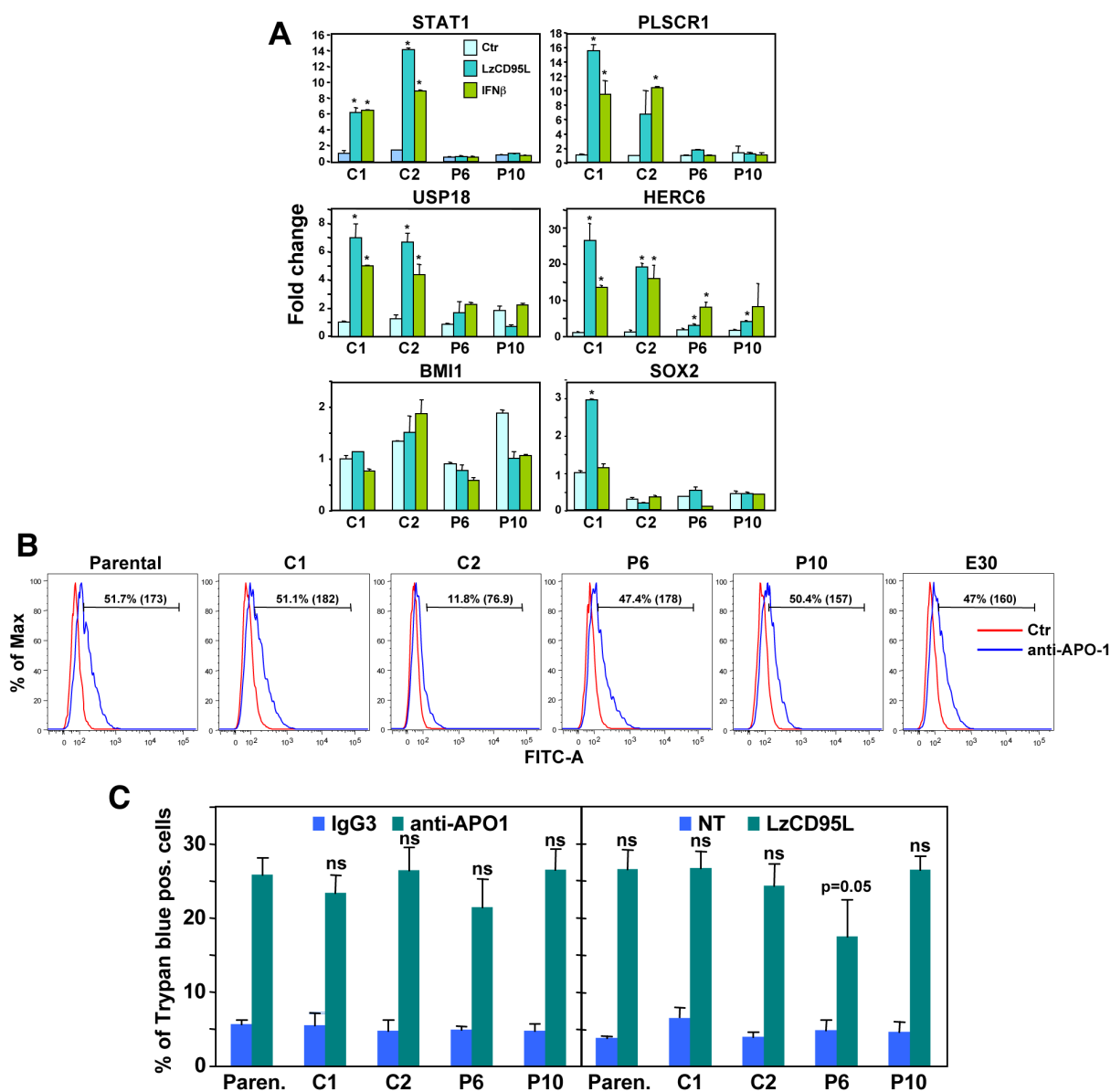


**Figure S8, related to Figure 6: Characterization of the STAT1 k.o. clones.**

(A) Real time PCR analysis of mRNAs of two Cas9 control clones (C1 and C2) and two STAT1 k.o. clones (P6 and P10) after a 4 day treatment with either LzCD95L or IFN $\beta$ . \* p-value < 0.05.

(B) Surface staining for CD95 in the parental MCF-7, Cas9 transfected and STAT1 k.o. clones. MFI is given in parenthesis.

(C) Sensitivity of the cells in A to CD95 mediated apoptosis 24 hrs after addition of either anti-APO-1 or LzCD95L. Significance of induced cell death is shown in the clones compared to the parental (Paren.) cells.

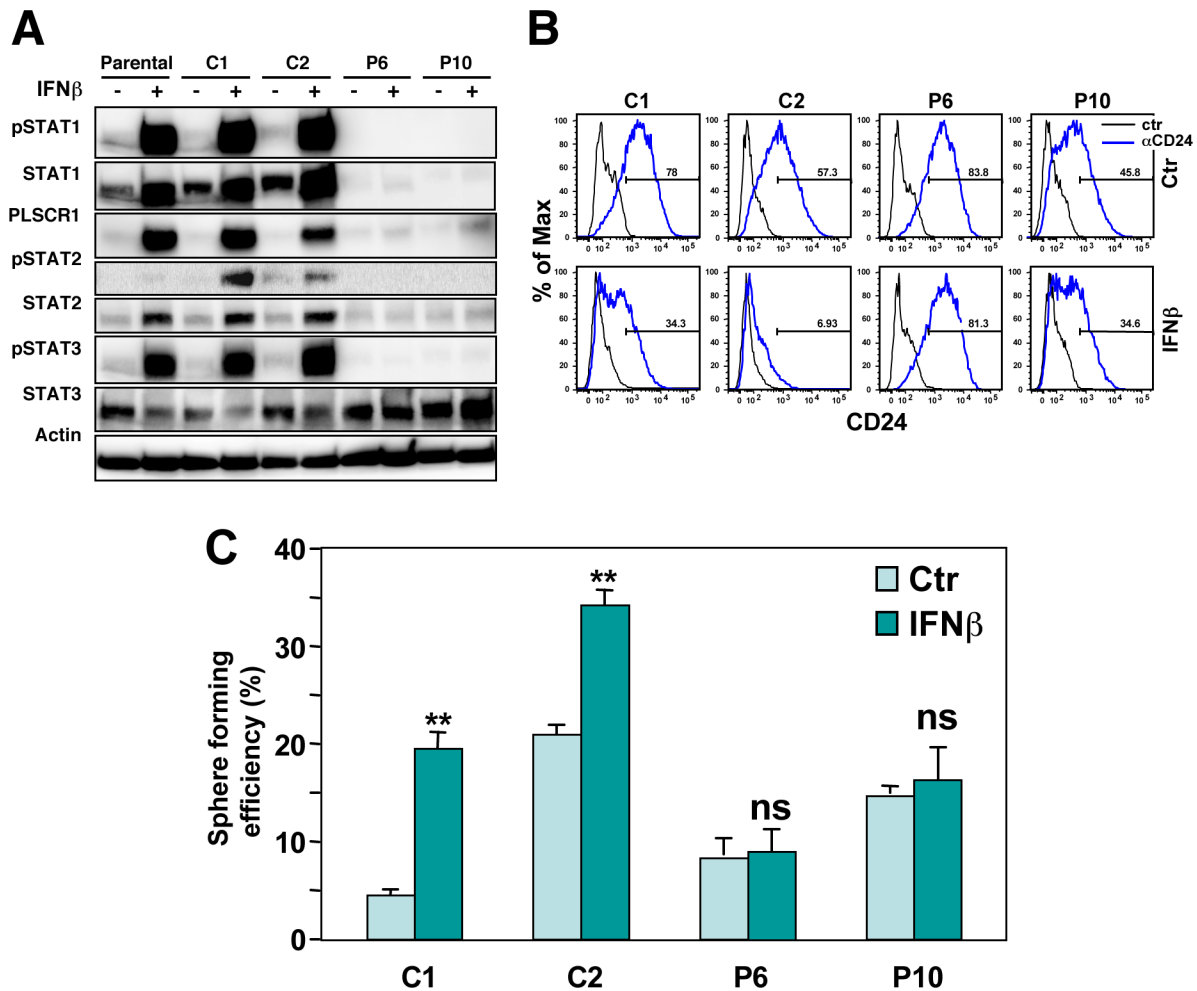


**Figure S9, related to Figure 6: Response of STAT1 k.o. cells to IFN $\beta$ .**

(A) Western blot analysis of MCF-7 cells, Cas9 transfected wt clones and STAT1 k.o. clones treated with IFN $\beta$  for 4 days.

(B) CD24 surface staining of the clones in A, either control treated or treated with IFN $\beta$  for 6 days.

(C) Percent of wells with spheres after plating MCF-7 cells, Cas9 transfected wt clones and STAT1 k.o. clones treated with either LzCD95L or IFN $\beta$  for 6 days at one cell per well in 96-well plates.

p-value \* $<0.05$ , \*\* $<0.001$ ; \*\*\* $<0.0001$ ; ns, not significant.

**Supplemental Tables:**

Table S1, related to Figure 1. All proteins that were up >1.5 in CD95 stimulated and down in shCD95L treated cells.

Table S2, related to Figure 3. Genes upregulated after CD95 stimulation.

Table S3, related to Figure 3. STAT1 specific ChIP-Seq Analysis in MCF-7 cells stimulated with anti-APO-1 for 10 days versus IgG treated cells.

Table S4, related to Discussion. Reanalysis of genes upregulated more than 1.5 fold in 2004 gene array of CD95 stimulated MCF-7(FB) cells (Barnhart et al., 2004).

Table S5, related to Method section. Quantitative proteomics data.

## Methods

**Cell Lines.** The breast cancer cell lines MCF-7, Hs578T, SK-BR3, T47D, HCC70, and the human melanoma cell line MDA-MB-435 were purchased from the ATCC. The head and neck squamous cell carcinoma line SCC-61 and its radiation-resistant variant Nu61 were described before (Khodarev et al., 2007). MCF-7, Hs578T, T47D, HCC70, and MDA-MB-435 were cultured in RPMI 1640 medium (Mediatech Inc) containing 10% heat-inactivated fetal bovine serum (FBS) (Sigma-Aldrich) and 1 % penicillin/streptomycin (Mediatech Inc). SCC61 and Nu61 cells were grown in DMEM/F-12 (1:1) (GIBCO) with 20% FBS and 1% penicillin–streptomycin, 0.4 µg/ml hydrocortisone (Sigma Aldrich). The SK-BR3 cell line was cultured in McCoy's 5A medium (ATCC) with 10% FBS and 1% penicillin–streptomycin. Mouse colon cancer CT26 cells, human CD95L expressing CT26 (CT26L) cells, MCF-7 cells overexpressing miR-ZIP anti-miRNA control or miR-ZIP200 (anti-miR-200c), MCF-7-pLenti-vector and MCF-7-pLenti-CD95L, were cultured as previously described (Ceppi et al., 2014). MCF-7-vec and MCF-7 cells reconstituted with caspase 3 (MCF-7(C3)) were grown in RPMI 1640 supplemented with 100 µg/ml G418 (Janicke et al., 1998). GSC20 is a cell line derived from a patient with the mesenchymal subtype of GBM grown as glioma sphere cultures as described (Bhat et al., 2013).

**Reagents and Antibodies.** Reagents used for Western blotting were obtained from the following sources (all primary antibodies were used at a 1:1000 dilution, unless otherwise specified): Anti-STAT1 (#9175), anti-pY701STAT1 (#9167), anti-pY727STAT1 (#8826), anti-STAT2 (#4594), anti-pY690STAT2 (#4441), anti-STAT3 (#4904), anti-pY705STAT3 (#9131), anti-SOX2 (#2748), anti-caspase-3 (#9662) were from Cell Signaling. The anti-hCD95L (#556387; 1:500) antibody were from BD Biosciences. To detect mouse STAT1 in CT26 and CT26L cells anti-STAT1 (ab-3987) from Abcam was used. Anti-hCD95 (sc-715, C-20), anti-STAT1 (for ChIP-Seq analysis, #sc-345), anti-PLSCR1 (sc-27779 1:500), anti-hCD24 (sc-58999, 1:200) and anti-hCD44 (sc-65265, 1:200) and HRP conjugated anti β-actin antibody (sc-47778; 1:5000), were from Santa Cruz Biotechnology. Blocking antibodies for IFNAR1 (clone MAR1-5A3, #04-151) and IFNAR2 (MAB1155) and membrane bound Fas Ligand (mCD95L #01-210) were from Millipore (Upstate). All secondary antibodies were used at 1:5000: goat anti-mouse IgG, HRP-conjugated, rabbit anti-goat IgG, HRP-conjugated, and goat anti-rabbit IgG, HRP-conjugated (Southern Biotech). Bovine serum albumin (BSA), puromycin, G418, protein A, propidium iodide and DMSO were from Sigma Aldrich. zVAD-fmk (BML-P416) caspase inhibitor (used at 20 µM) was from Enzo Lifesciences. Ruxolitinib (sc-36472) (used at 20 µM) was from Santa Cruz Biotechnology. IFNα (11200-1) (used at 2000 U/ml) and IFNβ (11415-1) (used at 1000 U/ml) were purchased from pbl Assay Science. Anti-CD95 mAb anti-APO-1, leucine zipper tagged CD95L (LzCD95L) were used to induce apoptosis at 100 ng/ml as described before unless otherwise specified (Ceppi et al., 2014). In all cases when anti-APO-1 or control IgG3 was used 1 ng/ml of Protein A (Sigma) was added to crosslink the antibodies. Cells treated with inhibitors were pretreated at least 1 hr before for any further treatment of anti-APO-1, LzCD95L, IFNα or IFNβ. Multiplicity of infection (MOI) for the CD95, STAT1 knockdown and pLKO

control particles (Sigma) was 3. For all conditions, cells were collected after 4 days after treatment except when otherwise noted.

### **SILAC Analysis.**

*Protein reduction, alkylation, and digestion.* Protein concentrations were measured using the BCA Protein Assay (Thermo Scientific, Rockford, IL). Reduction, alkylation, trypsin digestion, and desalt using C18 Sep-Pak cartridges were performed as previously described (Helou et al., 2013). A 5 pmol fraction of synthetic peptide Angiotensin II phosphate (DRVpYIHPPF) was added to each replicate and time point sample as an exogenous quantitation standard prior to Sep-Pak desalt.

*Automated nano-LC/MS.* A fully automated proteomic technology platform was implemented to analyze tryptic peptides as previously described (Yu and Salomon, 2009, 2010). The nanoLC-MS/MS experiments were performed with an Agilent 1200 Series Quaternary HPLC system (Agilent Technologies, Santa Clara, CA) connected to a Q Exactive mass spectrometer (Thermo Fisher Scientific, Waltham, MA). Peptides were eluted through a PicoFrit analytical column (360  $\mu\text{m}$  outer diameter 75  $\mu\text{m}$  inner diameter-fused silica with 12 cm of 3- $\mu\text{m}$  Monitor C18 particles; New Objective, Woburn, MA) with a reversed-phase gradient (0–70% 0.1M acetic acid in acetonitrile in 90 minutes). An electrospray voltage of 2 kV was applied using a split flow configuration. The Q Exactive was operated in the data dependent mode using a top-9 data dependent method. Survey full scan MS spectra ( $m/z$  400-1800) were acquired at a resolution of 70,000 with an AGC target value of  $3 \times 10^6$  ions or a maximum ion injection time of 200 ms. Peptide fragmentation was performed via higher-energy collision dissociation (HCD) with the energy set at 28 NCE. The MS/MS spectra were acquired at a resolution of 17,500, with a targeted value of  $2 \times 10^4$  ions or a maximum integration time of 250 ms. The underfill ratio, which specifies the minimum percentage of the target value likely to be reached at maximum fill time, was defined as 1.0%. The ion selection abundance threshold was set at  $8.0 \times 10^2$  with charge state exclusion of unassigned and  $z = 1$ , or 6-8 ions and dynamic exclusion time of 20 seconds.

*Database analysis* MS/MS spectra were searched against the non-redundant human UNIPROT "complete proteome set" database (UniProt; downloaded 2/1/2013) using MASCOT v. 2.4 (Matrix Science, Ltd, London W1U 7GB UK). A concatenated database containing 175,226 "target" and "decoy" reversed sequences was employed to estimate the FDR. Msconvert from ProteoWizard (v. 3.0.5047), using default parameters and with the MS2Deisotope filter on, was employed to create peak lists for Mascot. Mascot database searches were performed with the following parameters: trypsin enzyme cleavage specificity, 2 possible missed cleavages, 10 ppm mass tolerance for precursor ions, 20 mmu mass tolerance for fragment ions. Search parameters specified a differential modification of methionine oxidation (+15.9949 Da) as well as a static modification of carbamidomethylation (+57.0215 Da) on cysteine. Search parameters also included a differential modification for arginine and lysine (+6.0201 Da) amino acids. Mascot results were filtered by Mowse score ( $>20$ ). Peptide assignments from the database search was filtered down to 1% FDR by a logistic spectral score, as previously described (Yu et al., 2009). The mass spectrometry proteomics data have been deposited to the ProteomeXchange

Consortium via the PRIDE partner repository with the dataset identifier PXD004232 (username: reviewer58214@ebi.ac.uk, password: tTNCWdv8).

*Relative peptide abundance quantification.* Relative quantification of peptide abundance was performed through calculation of select ion chromatogram (SIC) peak areas. Retention time alignment of individual replicate analyses was performed as described previously (Demirkan et al., 2011). Peak areas were calculated by inspection of SICs using in-house software programmed in R 3.0 based on the Scripps Center for Metabolomics' XCMS package (version 1.40.0). This approach performed multiple passes through XCMS's central wavelet transformation algorithm (implemented in the centWave function) over increasingly narrower ranges of peak widths, and used the following parameters: mass window of 25 ppm, minimum peak widths ranging from 2 s to 20 s, maximum peak width of 80 s, signal to noise threshold of 10 and detection of peak limits via descent on the non-transformed data enabled. For cases when centWave did not identify an MS peak, we used the getPeaks function available in XCMS to integrate in a pre-defined region surrounding the maximum intensity signal of the SIC. SIC peak areas were determined for every peptide that was identified by MS/MS. In the case of a missing MS/MS for a particular peptide, in a particular replicate or treatment condition, SIC peak areas were calculated according to the peptide's theoretical mass and the retention time calculated from retention time alignment. A minimum SIC peak area equivalent to the typical spectral noise level of 1000 was required of all data reported for label-free quantitation. Individual SIC peak areas were normalized to the peak area of exogenously spiked peptide standard that was added in the same amount to each time point and replicate sample and accompanied peptides through enrichment and reversed-phase elution into the mass spectrometer.

$Q$  values for multiple hypothesis tests were calculated between the 6 replicate measurements for each peptide based on the determined paired  $p$  values using the R package QVALUE. A  $q$  value is defined as the measure of the minimum FDR at which a test can be called significant (Storey, 2002). All data was thresholded at  $Q$  value of 0.05 and fold change between treatment groups of  $>1.5$ . All of the identified peptides from every LCMS run are described in detail in **Table S1** and all quantitative data is provided in **Table S5**.

**ChIP-Seq Analysis.**  $1.5 \times 10^7$  treated cells (three biological replicates per condition) were collected from a 20 mm dish (80% confluent) and processed as previously described using an anti-STAT1 Ab (Yu et al., 2010). The binding of STAT1 on putative target genes in unstimulated cells was confirmed by qPCR with the following primers: RPS9-F:CGCCGGCGTTACTATAAGAG, RPS9-R: CATCCAACCCAAACCCTAGA, IFNAR2-F: CCGCTTCTGTCCGAGAGG, IFNAR2-R: GGCTCCCGAGAGATGCTA. ChIP-SEQ libraries were generated using a TruSeq ChIP Library Preparation Kit (Illumina, San Diego, CA) according to the Illumina provided protocol and sequenced on a HiSEQ2500 (Illumina, San Diego, CA). Sequence reads were aligned to the Human Reference Genome hg19 using Burrows-Wheeler Alignment Tool (BWA). Peak identification was performed using the Hypergeometric Optimization of Motif Enrichment Suite (Homer).

**Microarray Analyses.** To identify genes that are upregulated in MCF-7 cells long term stimulated through CD95 cells were treated with either isotope matched IgG3 or anti-APO-1 for 14 days. Total RNA was extracted (Qiagen kit) from  $1.5 \times 10^6$  treated cells (two biological replicates per condition). RNA samples at 250 ng/ $\mu$ l concentration were submitted to the Genome Core facility of Northwestern University and subjected to Nanodrop and Bioanalyzer analysis. Gene expression was determined using a HumanHT-12 v4 Expression BeadChip Kit following the manufacturers instructions. Data quality check was performed using Bioconductor Lumi package for R statistical programming environment. The data processing also included a normalization procedure utilizing quantile normalization method. Hierarchical clustering and Principal Component Analysis were performed on the normalized signal data to assess the sample relationship and variability. R software was used for data annotation and log2ratio calculation. Both the data on the ChIP-Seq and the gene array analyses were deposited at GEO under the series accession number GSE81860. A Lincscld analysis (lincscld.org) was performed against >1.4 million gene signatures with the genes up- or down regulated >1.5 after CD95 stimulation (see **Figure S3A**) using default settings.

Genes differentially expressed between SCC61 and Nu61 cells grown *in vivo* were described before and the data sets can be accessed at GEO (accession number GSE9713). Two independent data sets were analyzed: In both experiments (#1: GDS3124, #2: GDS3125) tumors were grown 2 to 3 weeks after injection to reach an average size of 400 mm<sup>3</sup> and three mice for each tumor (SCC61 and Nu61) were analyzed.

**Gene Set Enrichment Analysis (GSEA).** GSEA was performed using Broad Institute software with the GSEAPreranked analysis setting and default parameters (Mootha et al., 2003; Subramanian et al., 2005). Genes were ranked according to fold change in pre-specified pairwise comparisons (MCF-7 cells treated through CD95 vs. MCF7 treated with IgG3, and Nu61 vs. SCC61 tumors) and were evaluated with reference to the IFN sensitive genes (ISG) described elsewhere (Schoggins et al., 2011).

**Western Blot Analysis.** Cells were lysed and quantified as described previously (Ceppi et al., 2014). Proteins (20-50  $\mu$ g) in lysates were resolved on 10% SDS-PAGE gels and transferred to nitrocellulose membrane (Amersham Biosciences). The membranes were blocked with 5% BSA in 0.1% TBS/Tween-20 and incubated in primary antibodies diluted in blocking solution at 4°C overnight. After incubation with secondary antibodies, detection was performed using the ECL method (Thermo Scientific) and developed using a chemiluminescence imager, G:BOX Chemi XT4 (Syngene). Densitometry of Western blot bands was performed using the Syngene software package GeneTool.

**FACS Analysis.** Flow cytometry for CD24/CD44 staining, to determine ALDH1 activity and for CD95 surface staining were performed as previously described (Ceppi et al., 2014). CD95 surface staining for GSC20 was also done as previously described (Ceppi et al., 2014) and cell sorting was performed for CD95 high and CD95 low population using a Beckman Coulter

MoFlo sorter at the Flow Cytometry Core Facility of the Northwestern University.

For CD95/IFNAR1 double staining, cells were washed and resuspended in PBS with 3% BSA. Then, cells were stained with either 5  $\mu$ l FITC mouse IgG1 Kpa isotype control (BD Bioscience, #556640) and Mouse IgG1 R-PE conjugated negative control (Life Technologies, #GM4993) or FITC mouse anti-human CD95 (BD Bioscience, #551954) and IFNAR1 antibody PE-conjugated (Invitrogen, #MAB-23630) for 30 min at 4°C. Cells were washed twice and re-suspended in PBS and FACS analysis was performed on a Becton Dickinson LSR Fortessa. For CD95/IFNAR2 double staining, cells were washed twice in PBS with 3% BSA and stained with either mouse IgG2a Isotype control (BD Bioscience #555571) or IFNAR2 primary antibody (Millipore, #MAB1155) for 30 min at 4°C in the dark. Cells were then washed and centrifuged twice at 500g and incubated with secondary Alexa Fluor® 594 Goat Anti-Mouse IgG (Life Technologies #A-11005) antibody for 30 min. Cells were then washed twice and then incubated with either 5  $\mu$ l FITC mouse IgG1 Kpa isotype control (BD Bioscience, #556640) or FITC mouse anti-human CD95 (BD Bioscience, #551954) for an additional 30 min 4°C in the dark. Finally cells were washed twice and re-suspended in PBS and FACS analysis was performed.

**Sphere Forming Assays.** Cells were collected and washed with PBS. 40,000 cells were seeded in triplicate in each well on Ultra-Low attachment 6 well plates (Corning) in Mammocult cancer stem cell medium (Cell Stem Technology; prepared according to manufacturer's instructions). Spheres were counted using a light microscope 4 days after seeding.

An alternative protocol (modified from (Spike et al., 2012) was used to ensure that the spheres originated from single cells and not from cell aggregates. In brief, parental MCF-7, MCF-7 cas9 clones (C1 and C2), STAT1 k.o. clones (P6 and P10), or pLenti-vector and pLenti-STAT1 reconstituted P6 clones were pre-treated with IgG3, anti-APO-1, LzCD95L, IFN $\beta$ , or received no treatment for 6 days. Proper reprogramming was verified by FACS analysis for CD24/CD44 staining. Cell suspensions were passed through a 40 $\mu$ m sterile cell strainer (Fisher Scientific) to obtain single cells. The strained cell suspension was serially diluted in Mammocult media and seeded at 1 cell/well in triplicate in ultra-low adherence round bottom 96-well plates (Corning). The cells were cultured in Mammocult media supplemented with 4  $\mu$ g/ml Heparin, 0.5  $\mu$ g/ml hydrocortisone and 10% Mammocult Proliferation Supplement. After 6-7 days, cultures were scanned using IncuCyte Zoom and spheres were counted.

For RNA and protein isolation, 100,000 cells were plated either under adherent or sphere forming conditions, and after 4 days samples were collected or passaged and replated for 2 more generations of sphere formation. Cells were then harvested for protein quantification using Western blot or RNA quantification using qPCR.

**IFNAR Neutralization.** To block type 1 interferon signaling, MCF-7 cells were pretreated with 5  $\mu$ g/ml of either anti-IFNAR1 or anti-IFNAR2 antibodies or both for four hours and then treated LzCD95L for 4 days. Cells lysates were analyzed by western blotting.

**ELISA.**  $2.0 \times 10^5$  MCF-7 or SCC61 cells were seeded in 6 well plates and then treated with anti-APO-1 or LzCD95L for 48 hr. To inhibit caspases some samples were pretreated for 1 hr with 20



$\mu\text{M}$  of zVAD-fmk before adding anti-APO-1 or LzCD95L. Both cells and cell supernatant were harvested. Supernatants and cell lysates were purified by centrifugation and the protein level of cell lysate was measured and equal concentration applied to ELISA plates to quantify human IFN $\alpha$  (*Verikine*<sup>TM</sup> Human IFN $\alpha$  ELISA kit, pbl Assay Science) or human IFN $\gamma$  (R & D Systems) following the manufacturer's instructions.

**Quantitative Real-time PCR.** Total RNA was extracted using QIAzol Lysis reagent (Qiagen Sciences) and RNA concentration was measured using a NanoDrop 2000. 1  $\mu\text{g}$  of total RNA was used to generate cDNA using the High-Capacity cDNA ReverseTranscription Kit (Applied Biosystems). Gene expression was quantified using specific primers from Life technologies for *GAPDH* (Hs00266705\_g1), *STAT1* (Hs01013996\_m1), *PLSCR1* (Hs01062171\_m1), *HERC6* (Hs00215555\_m1), *USP18* (Hs00276441\_m1), *SOX2* (Hs01053049\_s1), *BMI1* (Hs00995521\_g1) and *ZEB1* (Hs00611018\_m1) using of the comparative  $\Delta\text{CT}$  method, and expressed as fold differences.

**Gene Silencing using Lentiviral shRNAs or siRNA.** The shRNA (shL3) used to knockdown hCD95L was described previously (Ceppi et al., 2014). To knockdown of hSTAT1, 150,000 MCF-7 cells seeded in 6 well plates were infected with the MISSION<sup>®</sup> Lentiviral Transduction Particles (Sigma): either pLKO.2-puro control transduction particle coding for a nontargeting (scrambled) shRNA (#SHC002) (CCGGCAACAAGATGAAGAGCACCAACTCGAGTTG GTGCTCTTCA TCTTGT TGTTTTT) or two shRNAs against mRNA NM\_007315 (Homo sapiens STAT1) TRCN0000280024 (CCGGCCCTGAAGTATCTGTATCCAACCTCGAGTT GGATACAGATACTTCAGGGTTTTTG) and TRCN0000004264 (CCGGGAACAGAAA TACACCTACGAACTCGAGTTCGTAGGTGTATTTCTGTTCTTTTT) at a M.O.I. of 3 in the presence of 8  $\mu\text{g}/\text{ml}$  polybrene. Cells were cultured in selection medium containing 3  $\mu\text{g}/\text{ml}$  of puromycin for two days. In all experiments involving puromycin selection, mock infected cells were included and were also treated with puromycin. Cells were only analyzed after all such non-infected cells died within 2-3 days after addition of puromycin. To knockdown hSTAT1 using siRNAs,  $1.0 \times 10^6$  MCF-7 cells were seeded in 100 mm plates one day prior to transfection. Cells were transfected with either 50 nM of a SMART pool of 4 mammalian nontargeting siRNAs (D-001810-10-20) (UGGUUUACAUGUCGACUAA, UGGUUUACAUGUUGUGU GA, UGGUUUACAUGUUUUCUGA, UGGUUUACAUGUUUUCUA) or the On-target siRNA SMART pool against human STAT1 (L-003543-00-0020) (GCACGAUGGGCUC AGCUUU, CUACGAACAUGACCCUAUC, GAACCUGACUCCAUGCGG, AGAAAGAG CUUGACAGUAA) using Dharmafect 2. After 24 hrs, the transfected cells were reseeded in 6 well plates for treatment. For the CD24/CD44 staining and Aldefluor assay MCF-7 cells were re-transfected with 50 nM of SMART pool of nontargeting or human STAT1 siRNAs after 3 days of treatment. SCC61 cells were directly cultured in 6 well plates and transfected 50 nM of SMART pool of nontargeting or human STAT1 siRNAs using Lipofectamine 2000 (Invitrogen).

**CRISPR/Cas9 Mediated Deletion of STAT1.** In order to generate STAT1 k.o. MCF-7 cells two gRNAs were designed (gRNA#1: AAGCTGGTGAACCTGCTCCAGG and gRNA#2: TCTTGCTACAGCATAACATAAGG) to delete a section covering part of exon 3 and exon 4 (the E deletion) and two gRNAs (gRNA#1: TTAGGGCCATCAAGTTCCATTGG and gRNA#2: GACGAGGTGTCTCGGATAGTGGG) to delete a section covering part of exon 23 and exon 24 that codes for a portion of STAT1 that contains both the Tyr701 and the Ser727 phosphorylation site (the P deletion). The entire DNA fragments were synthesized as gBlocks (U6 promoter + target sequence + guide RNA scaffold + termination signal) by IDT. gBlock pairs were transfected together with a Cas9 plasmid (pMJ920 plasmid coding for GFP) into  $2 \times 10^5$  MCF-7 cells using lypofectamin. To identify complete genomic deletions caused by gRNA pairs, genomic PCR was performed with a pair of primers (forward: 5-AGGCTGCCCTGATATGTT-3 and reverse: 5-TGTTCCCTGGAGCTTTAATGT-3 for the E deletion and forward: 5-GCCAGGCTAATGCCAATAAA-3 and reverse: 5-CGCATTCCGAAGAAAAACAT-3 for the P deletion). Two days after transfection, 10-20 % of cells that showed the highest GFP expression were sorted by FACS and expanded in 6 well plates. After 1-2 week cells were subjected to cell sorting at 1 cell per well directly into 96-well plates. After approximately two to three weeks, single cell clones were expanded and subjected to genotyping. Cells were also transfected with just the Cas9 plasmid and GFP positive cells subjected to single cell cloning (the C clones).

**Reconstitution of P6 and P10 STAT1 k.o. clones with STAT1.** A lentiviral vector expressing human wild-type STAT1 (pLV-WT-STAT1) was a gift from George Stark (Addgene plasmid # 71454) (Cheon and Stark, 2009). To generate viruses that express human wild-type STAT1, 3  $\mu$ g pCMVDR8.9 (packaging), 3  $\mu$ g pMD2.G (envelope), and 6  $\mu$ g of the lentiviral vector expressing human wild-type STAT1 (or empty vector as the control) were transfected in 293T cells using Lipofectamine 2000 (Invitrogen). Viruses were generated as described previously (Ceppi et al., 2014). The supernatant medium, either containing pLenti-vector control or pLenti-human STAT1 were collected after 48 h and, after filtering through 0.22  $\mu$ m syringe filter (Millipore), was used to infect STAT1 k.o. clones (P6 & P10) with 8  $\mu$ g/ml polybrene. Selection was done with 3  $\mu$ g/mL puromycin for more than 2 weeks.

**Orthotopic Growth of MCF-7 Cells in NGS Mice.** MCF-7 Cas9 clones (C1 & C2) and homozygous P-STAT1 k.o. clones (P6 & P10) were infected with pFU-L2G luciferase lentivirus as previously described (Ceppi et al., 2014). Then cells were treated with either IgG3 or anti-APO-1 for 9 days. MCF-7-C1/C2 (1:1) or MCF-7-P6/P10 (1:1) cell pools either treated with IgG3 or anti-APO-1 were injected into the fourth mammary fat pad at the base of the nipple into 6 weeks old female NOD-scid-gamma (NSG) mice (Jackson lab) according to the Northwestern University Institutional Animal Care and Use Committee (IACUC)-approved protocol. For each *in vivo* experiment, cancer cells were mixed with an equal volume of Matrigel (Cat#3432-010-01, Trevigen) in a total volume of 100  $\mu$ l. We also subcutaneously implanted a 17 $\beta$ -Estradiol pellet (Cat#SE-121, Innovative Research of America) into each mouse 1 day before cell injection. To determine tumor-initiating capacity MCF-7 cells, mice were injected with 10,000 or 1,000 pFU-

L2G luciferase-infected MCF-7 cells pretreated with either IgG3, anti-APO-1, or IFN $\beta$  pretreatment for 9 days. Growth of tumors was monitored weekly by using the IVIS Spectrum *in vivo* imaging system and luminescence was quantified at the regions of interest (ROI = the same area for each mouse encompassing the entire mammary gland) using the Living Image software.

**Primary Breast Cancer Cells.** Patient-derived breast tumor xenografts (Liu et al., 2010) were dissected from NOD/SCID mice with autoclaved scissors and forceps, and placed onto a 10 cm-petri dish in cold RPMI-1640 (Invitrogen) with 20 mM Hepes (Invitrogen) on ice. Tumor pieces were minced into fine pieces (1-3 mm<sup>3</sup>) with razor blades. 600  $\mu$ l of fresh Collagenase III (3000 units/ml in HBSS, Worthington Biomedical) and 100 Kunitz units of DNase I (D4263; Sigma-Aldrich, St. Louis) were added to the dish with fifteen ml of RPMI-1640 with 20 mM Hepes for tumor dissociation at 37°C with repeated pipetting/mixing every 15-20 minutes. After 2-3 hours, collected cell suspension were filtered using 40  $\mu$ m-nylon strainers and washed with RPMI-1640 with 10% calf serum (HyClone, Logan, UT). Cell pellet was resuspended in 5 ml of ACK lysis buffer (Invitrogen 1372) and incubated for 2 minutes on ice to lyse red blood cells and the cells were 10 volume washed with the Hanks' balanced saline solution (HBSS; BioWhittaker) with 2% heat-inactivated FBS. Cells were spun down (1200rpm, 5min, 4°C ) and resuspended in HBSS with 2% FBS at usually 10 million cells per ml.

*Tumor cell sorting.* Tumor cells were stained with human CD44 and mouse H2K<sup>d</sup> antibodies (BD) prior to flow sorting. CD44<sup>+</sup>H2K<sup>d-</sup> and CD44<sup>-</sup>H2K<sup>d-</sup> cells were collected in HBSS/20% FCS and cell pellets were utilized for proteomics analyses or resuspended in Trizol (Invitrogen) for RNA extractions.

*Mass spectrometry.* Cell pellets were lysed with 2% SDS and protease inhibitor cocktail and proteins were extracted using pulse sonification, followed up by filter-aided sample preparation (FASP) to clean up detergents. Upon LysC/Trypsin digestion, 500 ng proteins were analyzed via 4 hour LC/MS/MS method and data processed using Scaffold at Case Western Proteomics Core facility. Fold change was calculated based on total unique spectrum counts.

**Cell Growth/Proliferation Assay.** To follow cell proliferation in different cell populations pretreated with IgG3 or anti-APO-1 for 9 days, MCF-7 cell pools of C1/C2 or P6/P10 clones were seeded at 1000 cells/well in 96 well plates. Cell growth was monitored in quadruplicate samples at various time points using a confluency mask in an IncuCyte Zoom.

**Cell Death Assays.** To quantify cell death in parental or different Cas9 and STAT1 k.o. clones, 150,000 cells were plated in 12 well plates in triplicate and then either left untreated or treated with IgG3, anti-APO-1 or LzCD95L for 24 hr. Cells were resuspended in media and an equal volume of Trypan blue solution (Lonza) was added. Both living and dead (blue) cells were counted on a hemocytometer under a light microscope.

**Statistical Analysis.** All experiments were performed in triplicate. The results were expressed as mean  $\pm$  SD and analyzed by the Student's two-tailed t test or by ANOVA (Stata14). Statistical significance was defined as  $p < 0.05$ .

**References to Figure 1B:** (Blanco et al., 2011; Buday and Downward, 2007; Chang et al., 2012; Chung et al., 2011; Hsiao et al., 2013; Kainov et al., 2014; Kume et al., 2014; Lin et al., 2013; Pandey et al., 2011; Robinson et al., 2013; Schulz et al., 2009; Wu et al., 2014; Zhang et al., 2005).

## Supplemental References

- Barnhart, B.C., Legembre, P., Pietras, E., Bubici, C., Franzoso, G., and Peter, M.E. (2004). CD95 ligand induces motility and invasiveness of apoptosis-resistant tumor cells. *EMBO J* 23, 3175-3185.
- Bhat, K.P., Balasubramaniyan, V., Vaillant, B., Ezhilarasan, R., Hummelink, K., Hollingsworth, F., Wani, K., Heathcock, L., James, J.D., Goodman, L.D., *et al.* (2013). Mesenchymal differentiation mediated by NF-kappaB promotes radiation resistance in glioblastoma. *Cancer Cell* 24, 331-346.
- Blanco, M.A., Aleckovic, M., Hua, Y., Li, T., Wei, Y., Xu, Z., Cristea, I.M., and Kang, Y. (2011). Identification of staphylococcal nuclease domain-containing 1 (SND1) as a Metadherin-interacting protein with metastasis-promoting functions. *J Biol Chem* 286, 19982-19992.
- Buday, L., and Downward, J. (2007). Roles of cortactin in tumor pathogenesis. *Biochim Biophys Acta* 1775, 263-273.
- Ceppi, P., Hadji, A., Kohlhapp, F., Pattanayak, A., Hau, A., Xia, L., Liu, H., Murmann, A.E., and Peter, M.E. (2014). CD95 and CD95L promote and protect cancer stem cells. *Nature Commun* 5, 5238.
- Chang, S.H., Hong, S.H., Jiang, H.L., Minai-Tehrani, A., Yu, K.N., Lee, J.H., Kim, J.E., Shin, J.Y., Kang, B., Park, S., *et al.* (2012). GOLGA2/GM130, cis-Golgi matrix protein, is a novel target of anticancer gene therapy. *Mol Ther* 20, 2052-2063.
- Cheon, H., and Stark, G.R. (2009). Unphosphorylated STAT1 prolongs the expression of interferon-induced immune regulatory genes. *Proc Natl Acad Sci U S A* 106, 9373-9378.
- Chung, K.Y., Cheng, I.K., Ching, A.K., Chu, J.H., Lai, P.B., and Wong, N. (2011). Block of proliferation 1 (BOP1) plays an oncogenic role in hepatocellular carcinoma by promoting epithelial-to-mesenchymal transition. *Hepatology* 54, 307-318.
- Demirkan, G., Yu, K., Boylan, J.M., Salomon, A.R., and Gruppuso, P.A. (2011). Phosphoproteomic profiling of in vivo signaling in liver by the mammalian target of rapamycin complex 1 (mTORC1). *PLoS One* 6, e21729.
- Helou, Y.A., Nguyen, V., Beik, S.P., and Salomon, A.R. (2013). ERK positive feedback regulates a widespread network of tyrosine phosphorylation sites across canonical T cell signaling and actin cytoskeletal proteins in Jurkat T cells. *PLoS One* 8, e69641.
- Hsiao, K.C., Shih, N.Y., Fang, H.L., Huang, T.S., Kuo, C.C., Chu, P.Y., Hung, Y.M., Chou, S.W., Yang, Y.Y., Chang, G.C., *et al.* (2013). Surface alpha-enolase promotes extracellular matrix degradation and tumor metastasis and represents a new therapeutic target. *PLoS One* 8, e69354.
- Janicke, R.U., Ng, P., Sprengart, M.L., and Porter, A.G. (1998). Caspase-3 is required for alpha-fodrin cleavage but dispensable for cleavage of other death substrates in apoptosis. *J Biol Chem* 273, 15540-15545.
- Kainov, Y., Favorskaya, I., Delektorskaya, V., Chemeris, G., Komelkov, A., Zhuravskaya, A., Trukhanova, L., Zueva, E., Tavitian, B., Dyakova, N., *et al.* (2014). CRABP1 provides high malignancy of transformed mesenchymal cells and contributes to the pathogenesis of mesenchymal and neuroendocrine tumors. *Cell Cycle* 13.
- Khodarev, N.N., Minn, A.J., Efimova, E.V., Darga, T.E., Labay, E., Beckett, M., Mauceri, H.J., Roizman, B., and Weichselbaum, R.R. (2007). Signal transducer and activator of transcription 1 regulates both cytotoxic and prosurvival functions in tumor cells. *Cancer Res* 67, 9214-9220.

- Kume, H., Muraoka, S., Kuga, T., Adachi, J., Narumi, R., Watanabe, S., Kuwano, M., Kodera, Y., Matsushita, K., Fukuoka, J., *et al.* (2014). Discovery of colorectal cancer biomarker candidates by membrane proteomic analysis and subsequent verification using selected reaction monitoring and tissue microarray analysis. *Mol Cell Proteomics* *13*, 1471-1484.
- Lin, H.C., Zhang, F.L., Geng, Q., Yu, T., Cui, Y.Q., Liu, X.H., Li, J., Yan, M.X., Liu, L., He, X.H., *et al.* (2013). Quantitative proteomic analysis identifies CPNE3 as a novel metastasis-promoting gene in NSCLC. *J Proteome Res* *12*, 3423-3433.
- Liu, H., Patel, M.R., Prescher, J.A., Patsialou, A., Qian, D., Lin, J., Wen, S., Chang, Y.F., Bachmann, M.H., Shimono, Y., *et al.* (2010). Cancer stem cells from human breast tumors are involved in spontaneous metastases in orthotopic mouse models. *Proc Natl Acad Sci U S A* *107*, 18115-18120.
- Mootha, V.K., Lindgren, C.M., Eriksson, K.F., Subramanian, A., Sihag, S., Lehar, J., Puigserver, P., Carlsson, E., Ridderstrale, M., Laurila, E., *et al.* (2003). PGC-1 $\alpha$ -responsive genes involved in oxidative phosphorylation are coordinately downregulated in human diabetes. *Nat Genet* *34*, 267-273.
- Pandey, P.R., Okuda, H., Watabe, M., Pai, S.K., Liu, W., Kobayashi, A., Xing, F., Fukuda, K., Hirota, S., Sugai, T., *et al.* (2011). Resveratrol suppresses growth of cancer stem-like cells by inhibiting fatty acid synthase. *Breast Cancer Res Treat* *130*, 387-398.
- Robinson, T.J., Pai, M., Liu, J.C., Vizeacoumar, F., Sun, T., Egan, S.E., Datti, A., Huang, J., and Zacksenhaus, E. (2013). High-throughput screen identifies disulfiram as a potential therapeutic for triple-negative breast cancer cells: interaction with IQ motif-containing factors. *Cell Cycle* *12*, 3013-3024.
- Schoggins, J.W., Wilson, S.J., Panis, M., Murphy, M.Y., Jones, C.T., Bieniasz, P., and Rice, C.M. (2011). A diverse range of gene products are effectors of the type I interferon antiviral response. *Nature* *472*, 481-485.
- Schulz, D.M., Bollner, C., Thomas, G., Atkinson, M., Esposito, I., Hofler, H., and Aubele, M. (2009). Identification of differentially expressed proteins in triple-negative breast carcinomas using DIGE and mass spectrometry. *J Proteome Res* *8*, 3430-3438.
- Spike, B.T., Engle, D.D., Lin, J.C., Cheung, S.K., La, J., and Wahl, G.M. (2012). A mammary stem cell population identified and characterized in late embryogenesis reveals similarities to human breast cancer. *Cell Stem Cell* *10*, 183-197.
- Storey, J.D. (2002). A direct approach to false discovery rates. *J. R. Statist. Soc. B* *64*, 497-498.
- Subramanian, A., Tamayo, P., Mootha, V.K., Mukherjee, S., Ebert, B.L., Gillette, M.A., Paulovich, A., Pomeroy, S.L., Golub, T.R., Lander, E.S., *et al.* (2005). Gene set enrichment analysis: a knowledge-based approach for interpreting genome-wide expression profiles. *Proc Natl Acad Sci U S A* *102*, 15545-15550.
- Wu, H., Wang, K., Liu, W., and Hao, Q. (2014). PTEN overexpression improves cisplatin-resistance of human ovarian cancer cells through upregulating KRT10 expression. *Biochem Biophys Res Commun* *444*, 141-146.
- Yu, J., Yu, J., Mani, R.S., Cao, Q., Brenner, C.J., Cao, X., Wang, X., Wu, L., Li, J., Hu, M., *et al.* (2010). An integrated network of androgen receptor, polycomb, and TMPRSS2-ERG gene fusions in prostate cancer progression. *Cancer Cell* *17*, 443-454.
- Yu, K., Sabelli, A., DeKeukelaere, L., Park, R., Sindi, S., Gatsonis, C.A., and Salomon, A. (2009). Integrated platform for manual and high-throughput statistical validation of tandem mass spectra. *Proteomics* *9*, 3115-3125.
- Yu, K., and Salomon, A.R. (2009). PeptideDepot: flexible relational database for visual analysis of quantitative proteomic data and integration of existing protein information. *Proteomics* *9*, 5350-5358.

- Yu, K., and Salomon, A.R. (2010). HTAPP: high-throughput autonomous proteomic pipeline. *Proteomics* *10*, 2113-2122.
- Zhang, D., Tai, L.K., Wong, L.L., Chiu, L.L., Sethi, S.K., and Koay, E.S. (2005). Proteomic study reveals that proteins involved in metabolic and detoxification pathways are highly expressed in HER-2/neu-positive breast cancer. *Mol Cell Proteomics* *4*, 1686-1696.